sustainability

MDPI

Article

An Optimization Strategy for EV-Integrated Microgrids Considering Peer-to-Peer Transactions

Sen Tian [1], Qian Xiao [1,2,*], Tianxiang Li [1], Yu Jin [1], Yunfei Mu [1], Hongjie Jia [1], Wenhua Li [2], Remus Teodorescu [3] and Josep M. Guerrero [4]

[1] Key Laboratory of Smart Grid of Ministry of Education, Tianjin University, Tianjin 300072, China; ts_2022@tju.edu.cn (S.T.); txl@tju.edu.cn (T.L.); yu_jin@tju.edu.cn (Y.J.); yunfeimu@tju.edu.cn (Y.M.); hjjia@tju.edu.cn (H.J.)
[2] State Key Laboratory of Reliability and Intelligence of Electrical Equipment, Hebei University of Technology, Tianjin 300130, China; liwenhua@hebut.edu.cn
[3] Department of Energy Technology, Aalborg University, 9220 Aalborg, Denmark; ret@et.aau.dk
[4] Department of Electronic Engineering, Technical University of Catalonia, 08019 Barcelona, Spain; josep.m.guerrero@upc.edu
* Correspondence: xiaoqian@tju.edu.cn

Abstract: The scale of electric vehicles (EVs) in microgrids is growing prominently. However, the stochasticity of EV charging behavior poses formidable obstacles to exploring their dispatch potential. To solve this issue, an optimization strategy for EV-integrated microgrids considering peer-to-peer (P2P) transactions has been proposed in this paper. This research strategy contributes to the sustainable development of microgrids under large-scale EV integration. Firstly, a novel cooperative operation framework considering P2P transactions is established, in which the impact factors of EV charging are regarded to simulate its stochasticity and the energy trading process of the EV-integrated microgrid participating in P2P transactions is defined. Secondly, cost models for the EV-integrated microgrid are established. Thirdly, a three-stage optimization strategy is proposed to simplify the solving process. It transforms the scheduling problem into three solvable subproblems and restructures them with Lagrangian relaxation. Finally, case studies demonstrate that the proposed strategy optimizes EV load distribution, reduces the overall operational cost of the EV-integrated microgrid, and enhances the economic efficiency of each microgrid participating in P2P transactions.

Keywords: EV-integrated microgrid; peer-to-peer transactions; renewable energy; Lagrange relaxation; dispatch optimization; multi agent; cooperative operation; demand response; energy interaction; time-sharing tariff

Citation: Tian, S.; Xiao, Q.; Li, T.; Jin, Y.; Mu, Y.; Jia, H.; Li, W.; Teodorescu, R.; Guerrero, J.M. An Optimization Strategy for EV-Integrated Microgrids Considering Peer-to-Peer Transactions. *Sustainability* **2024**, *16*, 8955. https://doi.org/10.3390/su16208955

Academic Editor: Antonio Formisano

Received: 1 September 2024
Revised: 24 September 2024
Accepted: 8 October 2024
Published: 16 October 2024

1. Introduction

With the impetus from carbon neutrality and carbon peaking policies, the EV industry has experienced rapid growth [1–3]. By 2024, the market share of new energy EVs in the passenger vehicle sector has exceeded 50% and continues to rise. Large-scale EV grid integration, accompanied by disorderly charging loads, poses challenges to the sustainable development of microgrids and the balance of energy supply and demand [4,5]. Unlike the single microgrid, the multi-microgrid system can leverage energy transactions to activate flexible resources within each microgrid, creating greater dispatch potential for integrating EV loads [6]. Currently, many researchers are studying the optimization scheduling of EVs in microgrids and the operational strategies for interconnected microgrids.

In terms of the optimization scheduling of EVs within the microgrid, most research primarily focuses on optimizing EV load management to enhance user benefits and system security before integrating these loads into microgrid scheduling. Ref. [7] proposes a heuristic operation strategy for commercial building microgrids, which allows for the dynamic adjustment of EV charging and discharging power in response to changes in the

State of Charge (SOC) of EV batteries and photovoltaic (PV) output, utilizing a real-time event-triggered mechanism. Ref. [8] presents a detailed model of EV charging stations integrated into microgrids. This model has been tested in several real-world case studies and has proven capable of ensuring continuous and cost-effective power supply during grid failures, even under varying weather conditions. Ref. [9] proposes an improved Cross-Entropy algorithm to address the active and reactive power dispatch problem in microgrids that incorporate renewable energy and electric vehicles. Ref. [10] addresses the robust scheduling of electric vehicle charging in microgrids under worst-case wind power scenarios. A strategy improvement method based on robust simulation is developed, and its effectiveness is validated with real-world data. Ref. [11] proposes a low-complexity electric vehicle scheduling algorithm to balance time-aware fairness and overall waiting time. The method effectively reduces the total waiting time, minimizes individual waiting times, and lowers charging station operational costs. Ref. [12] proposes an electric vehicle charging scheduling strategy based on a cooperative hierarchical multi-agent system aimed at establishing a coordination mechanism between system operators and electric vehicle aggregators. Ref. [13] proposes an online electric vehicle charging and discharging strategy based on real-time electricity prices, designed to minimize the total charging costs and peak demand. Ref. [14] introduces a dynamic, real-time, demand-responsive energy pricing mechanism designed to allocate billing strategies for electric vehicle charging accurately and fairly. The literature above has established robust EV load management models. However, with large-scale EVs integrated into the grid, the stochasticity of EV charging behavior increases the difficulty of their control, making it challenging for microgrids to conduct real-time and effective scheduling.

In terms of operational strategies for interconnected microgrids, most research has developed multi-agent interest models for microgrid clusters, concentrating on energy trading strategies within the electricity market. Ref. [15] introduces a novel topology-aware multi-task reinforcement learning approach for the real-time coordination of local multi-energy microgrid clusters, with the goal of achieving system-wide load recovery. Ref. [16] proposes an energy management strategy based on distributed robust model predictive control to mitigate the adverse effects of uncertain renewable energy outputs in islanded multi-microgrid systems. Ref. [17] integrates plug-in electric vehicles and fuel cell electric vehicles within microgrids and develops a decentralized market-clearing model that allows neighboring microgrid clusters to interact within the local energy market. Ref. [18] integrates urban transportation networks into the optimal energy scheduling of multi-microgrid systems. It establishes a multi-period traffic distribution optimization model, allowing each microgrid to trade energy with other microgrids and utilize its fast-charging stations for electric vehicle charging. Ref. [19] combines model predictive control with approximate dynamic programming to study the multi-stage real-time stochastic operation of grid-connected multi-energy microgrids. Ref. [20] develops a distributed robust optimization algorithm based on the Wasserstein distance. This approach addresses optimization challenges arising from uncertainties in real-time electricity prices, renewable energy, loads, and electric vehicles in multi-microgrid systems. Ref. [21] models multi-energy microgrids as virtual power plants and, by incorporating Stackelberg game theory and integrated demand response, proposes an optimal operation strategy for multi-microgrids participating in the ancillary services market. Ref. [22] develops an energy-sharing strategy based on a transactive energy mechanism to coordinate interconnected multi-energy microgrids within regional integrated energy systems. The strategy leverages stochastic programming to account for the uncertainties in renewable energy and load demands. Ref. [23] proposes a parallel distributed optimization method for multi-microgrid energy management, designed to enhance the convergence speed without compromising the accuracy of the optimal solution. The literature above has demonstrated that interconnecting microgrid clusters can enhance overall economic efficiency. However, as the scale of EV loads grows, the availability of distributed resources within each microgrid increases, necessitating efficient cooperative integration strategies.

Based on the above analysis, an optimization strategy for the EV-integrated microgrid considering P2P transactions has been proposed. The primary contributions of this article can be outlined in the following three aspects:

(1) A novel cooperative operation framework for multiple interconnected EV-integrated microgrids is established, which outlines the impact factors for integrating EV loads into microgrid operations and the energy trading process among multiple microgrids.
(2) A multi-microgrid interaction strategy is proposed to simplify the solving process, transforming the energy-sharing and -trading problem into the following three solvable subproblems: minimizing EV load costs, minimizing multi-microgrid costs, and optimizing the distribution of interaction benefits.
(3) The objective functions of the three subproblems are reconstructed using Lagrange multipliers, and a three-stage optimization scheduling algorithm is employed to obtain the operating solution, ensuring both economic efficiency and safety in the operation of the EV-integrated microgrid.

The following is the outline of the upcoming sections of this paper: Section 2 establishes the cooperative operation framework and models multiple interconnected EV-integrated microgrids. Section 3 establishes cost models of the EV-integrated microgrid considering P2P transactions. Section 4 introduces the three-stage optimization scheduling strategy for the framework. Section 5 discusses the simulation results. Finally, conclusions are drawn in Section 6.

2. Cooperative Operation Framework and Models for Multiple Interconnected EV-Integrated Microgrids

This paper investigates the optimization of operational issues related to EV-integrated microgrids. To achieve this, we first introduce the development trends of EV-integrated microgrids within the context of the smart grid and subsequently establish its operational model.

2.1. Smart Grid Conceptual Diagram

This study is based on the concept of a smart grid, as illustrated in Figure 1. The smart grid can be structurally divided into the physical architecture and the functional architecture. The physical architecture comprises the following four key components: the source, network, load, and storage, which together manage the flow of energy. The functional architecture encompasses various service entities, enabling functions such as optimized scheduling, voltage regulation, and so on [24–28]. As the scale of EV loads within microgrids expands, their disorderly charging loads pose challenges to the energy supply–demand balance in microgrids. Therefore, this study focuses on the collaborative operation of multiple interconnected EV-integrated microgrids.

2.2. Operation Framework

Figure 2 illustrates the cooperative operation framework for multiple interconnected EV-integrated microgrids. The framework consists of a grid, a gas network, and several EV-integrated microgrids. The EV-integrated microgrid typically includes devices such as wind turbines (WT), PV, energy storage systems (ESS), combined heat and power units (CHP), gas boilers (GB), and information control centers, all of which ensure the energy supply and information transmission within the microgrid. The EV-integrated microgrid also includes various lower-level users, such as microgrid operators, EV users, ESS operators, and load operators.

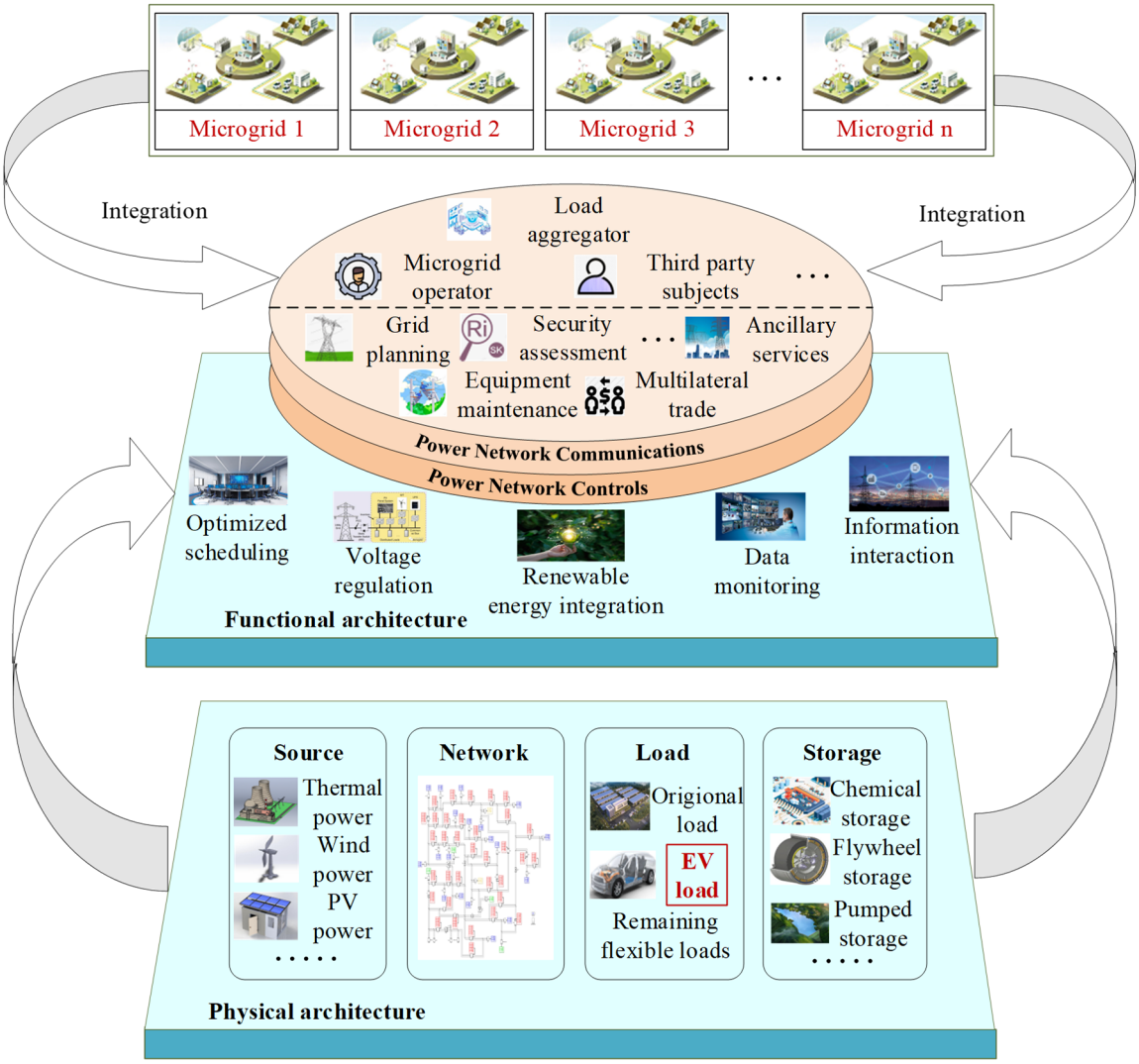

Figure 1. Smart grid conceptual diagram.

Collaboration among multiple interconnected EV-integrated microgrids aims for economic operation, and optimizing scheduling involves energy interactions between them. P2P transactions enable direct energy exchange without relying on a central authority, allowing participants to adjust energy exchange rules based on their own and others' needs [29–33]. Within this framework, microgrids can establish cooperative operating agreements, connecting through a common bus to facilitate energy trading, while also being able to sell internal energy to the grid. Each microgrid's internal scheduling is managed by operators through decentralized autonomy, participating in P2P transactions after reporting energy information.

P2P transactions within this framework between EV-integrated microgrids occur in three stages, as follows: minimizing EV load costs, minimizing multi-microgrid costs, and optimizing the distribution of interaction benefits. In the first stage, the EV-integrated microgrid performs distributed planning and optimization of the charging times and power of its EVs, then calculates the optimized EV charging load. In the second stage, all EV-integrated microgrids compute their own electricity demands and share this information with each other. Through information transmission, iterative optimization is conducted to determine the optimal energy exchange amounts between the microgrids. In the third stage, the energy trading prices between microgrids are formulated, with each microgrid communicating its desired trading prices based on energy exchange volumes, leading to an iterative determination of the optimal prices.

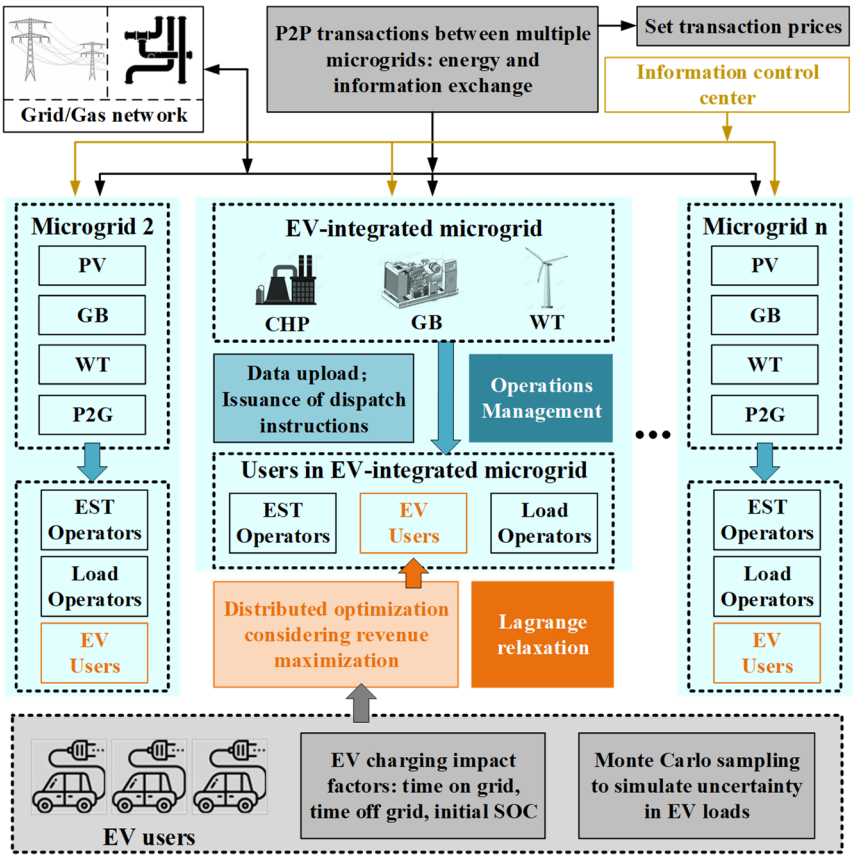

Figure 2. Cooperative operation framework for multiple interconnected EV-integrated microgrids.

2.3. Model of EV Users

Based on the findings provided in reference [34], a probabilistic distribution model is used to describe the commuting behavior of EV users within the EV-integrated microgrid, including travel times and distances. Monte Carlo sampling is employed to generate and extract commuting time data for EV users, which are then used to estimate the initial SOC values. This process results in the development of a charging load model for EV users.

The times at which EVs connect to the charging station follow a normal distribution, with the probability density function, as follows:

$$\begin{cases} f(t_{ar}) = \frac{1}{\sigma_{ar}\sqrt{2\pi}} \exp\left(-\frac{(j_{ar}+24-\mu_{ar})^2}{2\sigma_{ar}^2}\right) & 0 < j_{ar} \le \mu_{ar} - 12 \\ f(t_{ar}) = \frac{1}{\sigma_{ar}\sqrt{2\pi}} \exp\left(-\frac{(j_{ar}-\mu_{ar})^2}{2\sigma_{ar}^2}\right) & \mu_{ar} - 12 < j_{ar} \le 24 \end{cases} \quad (1)$$

where j_{ar} is the time when the EVs begin charging; and μ_{ar} and σ_{ar} are the mean and variance of the time when charging begins, respectively.

The times at which EVs disconnect from the charging station follow a normal distribution, with the probability density function, as follows:

$$\begin{cases} f(t_{le}) = \frac{1}{\sigma_{le}\sqrt{2\pi}} \exp\left(-\frac{(j_{le}+24-\mu_{le})^2}{2\sigma_{le}^2}\right) & 0 < j_{le} \le \mu_{le} - 12 \\ f(t_{le}) = \frac{1}{\sigma_{le}\sqrt{2\pi}} \exp\left(-\frac{(j_{le}-\mu_{le})^2}{2\sigma_{le}^2}\right) & \mu_{le} - 12 < j_{le} \le 24 \end{cases} \quad (2)$$

where j_{le} is the time when the EV finishes charging; and μ_{le} and σ_{le} are the mean and variance of the time when charging finishes, respectively.

This study assumes that the probability density function of EV travel distances follows a log-normal distribution. The model is specified as follows:

$$f(R_{dis}) = \frac{1}{\sigma_{dis} R_{dis} \sqrt{2\pi}} \exp\left(-\frac{(\ln R_{dis} - \mu_{dis})^2}{2\sigma_{dis}^2} \right) \tag{3}$$

where R_{dis} is the travel distance of EV; and μ_{dis} and σ_{dis} are the mean and variance of the travel distance, respectively. Thus, the initial SOC of the EV can be calculated using the following formula:

$$S_{in} = S_w - \frac{R_{dis} E_{per}}{C_{ba}} \tag{4}$$

where S_{in} and S_w are the initial SOC and the desired SOC set by the EV user, respectively; E_{per} is the consumed energy per unit distance traveled by the EV; and C_{ba} is the rated capacity of the EV battery. The EVs participating in the scheduling must simultaneously satisfy the following constraints:

$$S_{i,j+1}^{ev} = S_{i,j}^{ev} + P_{i,j+1}^{\mathrm{ev},c} \eta^c - P_{i,j+1}^{\mathrm{ev},d} / \eta^d \tag{5}$$

$$S_i^{\min} \le S_{i,j}^{ev} \le S_i^{\max} \tag{6}$$

$$0 \le P_{i,j}^{ev,c} \le P_{\max}^{ev,c} J_{i,j}^{ev,c} \tag{7}$$

$$0 \le P_{i,j}^{ev,d} \le P_{\max}^{ev,d} J_{i,j}^{ev,d} \tag{8}$$

$$J_{i,j}^{ev,c} + J_{i,j}^{ev,d} = J_{i,j}^{ev} \tag{9}$$

where $S_{i,j+1}^{ev}$ is the SOC of the EV i at time j; $P_{i,j+1}^{ev,c}$ and $P_{i,j+1}^{ev,d}$ are the charging and discharging power of the EV i at time $j+1$, respectively; η^c and η^d are the charging and discharging efficiencies of the EV, respectively; S_i^{min} and S_i^{max} are the minimum and maximum SOC values of the EV i, respectively; $P_{max}^{ev,c}$ and $P_{max}^{ev,d}$ are the maximum charging and discharging power of the EV, respectively; $J_{i,j}^{ev,c}$ and $J_{i,j}^{ev,d}$ are binary indicators for the EV's charging and discharging states at time j, where the values are either 0 or 1; and $J_{i,j}^{ev,'}$ is the status of the EV entering a charging station at time j, which it is 1 if the EV enters the station to charge, and 0 otherwise.

2.4. Models of ESS Operators and Devices

The model for energy storage devices within the microgrid is as follows:

$$\begin{cases} P_j^{ESS} = P_{j-1}^{ESS} + P_j^{ESS,c} \eta^{ESS,c} - P_j^{ESS,d} \eta^{ESS,d} \\ P_j^{ESS,c} \times P_j^{ESS,d} = 0 \end{cases} \tag{10}$$

where P_j^{ESS} is the output of ESS at time j; $P_j^{ESS,c}$ and $P_j^{ESS,d}$ are the charging and discharging power of ESS at time j, respectively; and $\eta^{ESS,c}$ and $\eta^{ESS,d}$ are the charging and discharging efficiencies of ESS, respectively.

The output model for renewable energy devices within the microgrid is as follows:

$$0 \le P_j^n \le P_j^{n,\max} \tag{11}$$

where n refers to the set {WT, PV}; P_j^n is the output of device n at time j; and $P_j^{n,max}$ is the maximum power of device n at time j.

The model for the energy conversion devices within the microgrid is as follows:

$$\begin{cases} P_j^{CHP} = \eta^{CHP} G_j^{CHP} \\ H_j^{CHP} = \eta^{CHP,h} P_j^{CHP} \\ H_j^{GB} = \eta^{GB,h} G_j^{GB} \end{cases} \tag{12}$$

$$\begin{cases} 0 \le P_j^{CHP} \le P^{CHP,\max} \\ 0 \le H_j^{GB} \le H^{GB,\max} \end{cases} \tag{13}$$

where P_j^{CHP} and H_j^{CHP} are the electrical and heat power outputs of the CHP at time j; G_j^{CHP} and G_j^{GB} are the gas consumption rates for the CHP and GB at time j, respectively; H_j^{GB} is the heat power output of the GB at time j; η^{CHP}, $\eta^{CHP,h}$, and $\eta^{GB,h}$ are the conversion efficiencies for the CHP electrical output, heat output, and GB heat output, respectively; and $P^{CHP,max}$ and $P^{GB,max}$ are the power output limits for the CHP and GB, respectively.

2.5. Model of Load Operators

In this paper, load operators manage the user loads within the EV-integrated microgrid, excluding EVs, and these loads can be adjusted based on DR. Based on references [35–38], this study considers two types of DR: incentive-based and substitute DR. The load model accounting for DR can be expressed as follows:

$$\begin{cases} L_j^{k,IDR} = L_j^{k,0} - \Delta L_j^{k,IBDR} - L_j^{k,SDR} \\ L_{j,\min}^{k,IDR} \le L_j^{k,IDR} \le L_{j,\max}^{k,IDR} \end{cases} \tag{14}$$

where k refers to the set $\{e, h\}$, where e stands for electricity and h stands for heat; $L_j^{k,0}$ and $L_j^{k,IDR}$ are the load of type k before and after DR at time j, respectively; $\Delta L_j^{k,IBDR}$ and $\Delta L_j^{k,SDR}$ are the adjustment amounts for load k under incentive-based and substitute DR mechanisms at time j, respectively; and $L_{j,max}^{k,IDR}$ and $L_{j,min}^{k,IDR}$ are the maximum and minimum values of load k after DR at time j.

3. Cost Models of an EV-Integrated Microgrid Considering P2P Transactions

EV-integrated microgrids participate in P2P transactions with transaction prices set by their operators, and the cost models for them are established as follows.

3.1. Operating Costs for an EV-Integrated Microgrid

The objective function for the EV-integrated microgrid considering P2P transactions is as follows:

$$C^{MG} = C^{EV} + C^{DE} + C^{DR} + C^{EX} + C^{WE} \tag{15}$$

where C^{MG} is the operating cost of the EV-integrated microgrid; C^{EV} is the energy consumption cost for EV users; C^{DE} is the operational and maintenance cost of the internal system device; C^{DR} is the DR cost; C^{EX} is the cost of energy interactions between the EV-integrated microgrid and other microgrids; and C^{WE} is the cost of energy interactions between the EV-integrated microgrid and the higher-level energy network.

We divide the day into T time periods, with each dispatchable EV having a duration of ΔT. The charging cost for EV users can be expressed as follows:

$$C^{EV} = \sum_{i=1}^{m} \sum_{j=1}^{T} \left(P_{i,j}^{ev,c} J_{i,j}^{ev,c} \lambda^{sell} - P_{i,j}^{ev,d} J_{i,j}^{ev,d} \lambda^{buy} \right) \tag{16}$$

where C^{EV} is the charging cost for EV users; λ^{sell} is the time-of-use electricity rate charged by the grid to EV users; and λ^{buy} is the fixed electricity price at which EV users supply power to the grid.

The EV-integrated microgrid can exchange electrical energy with other microgrids. The costs associated with these energy interactions are as follows:

$$C^{EX} = \sum_{i=1}^{n} \sum_{j=1}^{T} \left(\lambda_{i,j}^{ex} P_{i,j}^{ex} \right) \tag{17}$$

where n is the number of microgrids interacting with the EV-integrated microgrid; and $\lambda_{i,j}^{ex}$ and $P_{i,j}^{ex}$ are the energy interaction price and the amount of energy exchanged between the EV-integrated microgrid and microgrid i at time j, respectivley.

The transaction costs between the EV-integrated microgrid and the higher-level energy network are as follows:

$$C^{WE} = \sum_{j=1}^{T} \left(\lambda_j^{gas} P_j^{gas} + \lambda_j^{gr,buy} P_j^{gr,buy} - \lambda_j^{gr,sell} P_j^{gr,sell} \right) \tag{18}$$

where λ_j^{gas} and P_j^{gas} are the selling price of natural gas and the quantity of natural gas purchased by the EV-integrated microgrid at time j, respectively; $P_j^{gr,buy}$ and $P_j^{gr,sell}$ are the amount of electrical energy bought from and sold to the grid by the EV-integrated microgrid at time j, respectively; and $\lambda_j^{gr,buy}$ and $\lambda_j^{gr,sell}$ are the prices of buying and selling electrical energy from and to the grid at time j, respectively. The operating model for the remaining microgrid device in this paper is based on the research provided in references [39–41], and will not be detailed further here.

3.2. Power Balance and Constraints

The system's power balance and constraint conditions are as follows:

(1) Electrical Power Balance Constraints

$$P_j^{EX} + P_j^{WT} + P_j^{CHP} - L_j^{e,IDR} + P_j^{EST} + P_j^{WE} + P_j^{EV} = L_{e,j} \tag{19}$$

where $L_{e,j}$ is the electrical load of the microgrid at time j; P_j^{EX} is the net power of energy interaction between the EV-integrated microgrid and other microgrids at time j; P_j^{WT}, P_j^{CHP}, and P_j^{ESS} are the actual power outputs of WT, CHP, and ESS at time j, respectively; $L_j^{e,IDR}$ is the change in electrical load due to the IDR mechanism at time j; and P_j^{WE} is the net power of energy interaction between the EV-integrated microgrid and the grid at time j.

(2) Heat Power Balance Constraints

$$H_j^{GB} + H_j^{CHP} = L_{h,j} \tag{20}$$

where $L_{h,j}$ is the heat load of the microgrid at time j.

(3) P2P Energy Trading Constraints

$$\begin{cases} \left| P_{i,j}^{ex} \right| \le P_{i,j}^{ex,\max} \\ P_{1i,j}^{ex} + P_{i1,j}^{ex} = 0 \end{cases} \tag{21}$$

where $P_{i,j}^{ex,max}$ is the maximum amount of energy exchanged between the EV-integrated microgrid and microgrid i at time j. We consider the EV-integrated microgrid as Microgrid 1, where $P_{1i,j}^{ex}$ and $P_{i1,j}^{ex}$ are the power exchanged between Microgrid 1 and microgrid i at time j.

(4) EV Charging Constraints

In this study, it is assumed that, at any given time, when an EV connects to a charging station within the microgrid, the total EV load, along with all other current loads, does not exceed the maximum load capacity of the microgrid, as follows:

$$P_j^{EV} + L_{e0,j} \leq L^{\max} \tag{22}$$

where $L_{e0,j}$ is the grid load excluding the EV load at time j; and L^{max} is the maximum load that the EV-integrated microgrid can handle.

4. Three-Stage Optimization Scheduling Strategy for the Framework

The previous content has established the model for the EV-integrated microgrid and its interactions with other microgrids. Other microgrids also aim to reduce their costs during the trading process, necessitating a balance in the distribution of benefits during these interactions. The Nash bargaining model can select the most suitable operational strategy within a bounded, closed convex set of alternatives. Thus, the Nash bargaining model is introduced to facilitate negotiations between microgrids.

4.1. Three-Stage Subproblem Decomposition

The essence of Nash bargaining lies in ensuring that, after reaching an agreement or accepting unified management, the profits of all agents involved are higher than their respective profits when operating independently. The mathematical model for this is as follows:

$$\begin{cases} \sum_{i=1}^{n} \max\left(R_i^{af} - R_i^{be}\right) \\ s.t. \quad R_i^{af} \geq R_i^{be} \end{cases} \tag{23}$$

where n is the number of parties involved in the agreement; and R_i^{be} and R_i^{af} represent the benefits of agent i before and after the agreement, respectively. Based on the principle of Nash equilibrium, the optimization scheduling problem for the EV-integrated microgrid considering P2P transactions can be divided into three stages. It is important to note that this paper assumes that the charging stations within the microgrid are equipped with controllers that can record and optimize charging data for each EV.

(1) Stage 1: Minimizing EV load costs

For the EVs, the load optimization problem is transformed into a cost minimization problem. The mathematical model established above serves as the constraint conditions for the operational objectives at this stage, and the corresponding optimization problem is as follows:

$$\begin{cases} \min R_{ev} \\ s.t. \ \ formula(1)–(9)(16)(22) \end{cases} \tag{24}$$

where R_{ev} is the cost for EV users.

(2) Stage 2: Minimizing multi-microgrid costs

After optimizing the EV load, this study focuses on calculating the energy exchange between the EV-integrated microgrid and other microgrids, which involves minimizing the costs for both parties involved in the interaction.

$$\begin{cases} \min(R_{evi} + R_i) \\ s.t. \ \ formula(10)–(15)(17)–(20) \end{cases} \tag{25}$$

where R_{evi} is the energy cost for all EV-integrated microgrids; and R_i is the energy cost for the EV-integrated microgrid interacting with other microgrids.

(3) Stage 3: Optimizing the distribution of interaction benefits

A nonlinear function based on the natural logarithm is employed to quantify the contributions of different microgrids in energy sharing [42]. Subsequently, the microgrids negotiate with each other using their respective contributions as bargaining power, thereby determining the P2P energy transaction prices and fairly distributing the benefits of energy sharing, as follows:

$$\begin{cases} E_i^{su} = \sum_{j=1}^{T} \max\left(0, P_j^{ex}\right) \\ E_i^{re} = \sum_{j=1}^{T} \min\left(0, P_j^{ex}\right) \\ k_i = e^{E_i^{su}/E^{su,\max}} - e^{-E_i^{re}/E^{su,\max}} \end{cases} \tag{26}$$

$$\begin{cases} \min\left(C^{MG} - C^0\right) \\ s.t.\ \ formula(16)(21) \end{cases} \tag{27}$$

where E_i^{su} and E_i^{re} are the total energy supplied and received by the EV-integrated microgrid when participating in P2P transactions, respectively; k_i is the influencing factor that quantifies the degree of contribution of the microgrid in P2P transactions; $E^{su,max}$ and $E^{re,max}$ are the maximum values of energy supplied and received by the EV-integrated microgrid; and C^0 denotes the operational cost of the EV-integrated microgrid when not participating in P2P transactions.

4.2. Three-Stage Optimization Scheduling Method

This paper uses a distributed optimization algorithm that relaxes the objective function using Lagrange multipliers to iteratively solve the three proposed subproblems. The solution process for these three subproblems is shown in Figure 3.

Specifically, the solution information from one subproblem is incorporated into the solution process of the next. The three corresponding Lagrangian relaxation problems are established as follows:

(1) Minimizing EV load costs

$$L_1 = R_{ev} + \sum_{j=1}^{T} \varphi_j^{P1}\left(P_j^{EV} + L_{e0,t} - L^{\max}\right) \tag{28}$$

where φ_j^{P1} is the Lagrange multiplier for the first subproblem at time j and $\varphi_j^{P1} > 0$. After solving the charging and discharging plans for each EV in the first round, subsequent iterations can refer to the method described in reference [42].

(2) Minimizing multi-microgrid costs

$$L_2 = R_{evi} + R_i + \sum_{i}^{n}\sum_{k}^{n}\sum_{j}^{T}\left[\varphi_j^{P2}\left(P_{ik,j}^{ex} + P_{ki,j}^{ex}\right) + \varphi^{p2}\left\|P_{ik,j}^{ex} + P_{ki,j}^{ex}\right\|_2^2\right] \tag{29}$$

where φ_j^{P2} is the value of the Lagrange multipliers for the second subproblem at time j; φ_j^{P2} is the penalty factor for the second subproblem; and $P_{ik,j}^{ex}$ is the interaction power between microgrid i and microgrid k at time j, $i \neq k$.

(3) Optimizing the distribution of interaction benefits

$$L_3 = -k_i \ln\left(C^{MG} - C^0\right) + \sum_{i}^{n}\sum_{k}^{n}\sum_{j}^{T}\left[\varphi_j^{P3}\left(\lambda_{ik,j}^{ex} + \lambda_{ki,j}^{ex}\right) + \varphi^{p3}\left\|\lambda_{ik,j}^{ex} + \lambda_{ki,j}^{ex}\right\|_2^2\right] \tag{30}$$

where φ_j^{P3} is value of the Lagrange multipliers for the third subproblem at time j; φ_j^{P3} is the penalty factor for the third subproblem at time j; and $\lambda_{ik,j}^{ex}$ is the price of interaction power between microgrid i and microgrid k at time j, $i \neq k$.

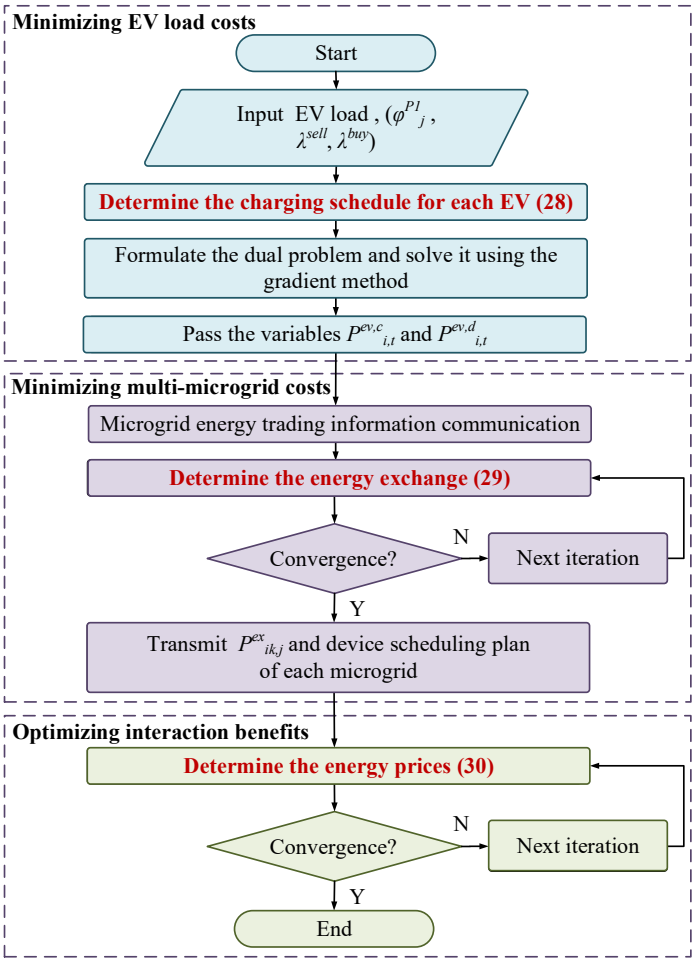

Figure 3. Solution process for the proposed three subproblems.

The alternating direction method of multipliers (ADMM) can decompose a complex global optimization problem into smaller subproblems, which can be solved independently by different entities. This decomposition allows each entity to focus solely on its local problem, thereby reducing the computational complexity. As a result, this algorithm is well suited for solving the three-stage subproblems presented in this paper.

5. Results and Discussions

The case study in this paper is validated using Matlab R2021a, its version number is 9.10.0.1602886.

5.1. Case Study

This study focuses on the framework established in Figure 2, investigating the participation of the EV-integrated microgrid considering P2P transactions. Two additional microgrid structures, similar in design to the research model—Microgrid 2 and Microgrid 3—are established for trading purposes. The energy supply equipment models are consistent with those in the EV-integrated microgrid model, but with fewer devices. The prices for microgrid electricity purchase, carbon emissions allowances, and natural gas procurement are shown in Table 1, while Figure 4 depicts the microgrid electric heating load curve and the output of WT for the EV-integrated microgrid. It is worth noting that some of the data in the examples are derived from the sources provided in references [30,31].

Table 1. Microgrid energy pricing information.

Type	Time	Price
Electricity sale (to grid)	The whole day	0.2/USD/kW
Gas purchase	The whole day	3.5/USD/m^3
Purchase of carbon credits	The whole day	0.425/USD/kg
Electricity purchase (from grid)	23:00–7:00	0.4/USD/kW
Electricity purchase (from grid)	8:00–11:00 15:00–18:00	0.75/USD/kW
Electricity purchase (from grid)	12:00–14:00 19:00–22:00	1.2/USD/kW

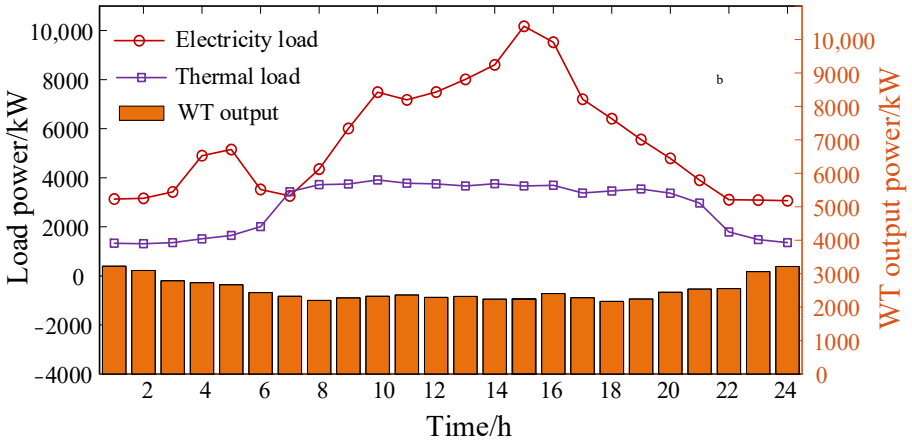

Figure 4. The microgrid electric heating load curve and the output of WT.

To validate the effectiveness of the proposed strategy for EV load management and the enhancement of microgrid operational efficiency, five cases have been established. These cases involve comparative analyses by varying both the management of EV loads and the control methods of the microgrid.

(1) Case 1: The EVs within the microgrid adopt an unregulated charging mode [34] without considering P2P transactions between microgrids and DR.
(2) Case 2: The EVs within the microgrid adopt an unregulated charging mode without considering P2P transactions between microgrids, but with consideration of DR.
(3) Case 3: The EVs within the microgrid adopt an unregulated charging mode with consideration of P2P transactions between microgrids and DR.
(4) Case 4: The EVs within the microgrid adopt an orderly charging mode without considering P2P transactions between microgrids, but with consideration of DR.
(5) Case 5: The EVs within the microgrid adopt an orderly charging mode with consideration of P2P transactions between microgrids and DR.

5.2. Impact of EV Dispatch

This study assumes that there are 100 EV users within the EV-integrated microgrid. Under the unregulated charging mode, the times when EVs connect to and disconnect from the charging station, as well as their driving distances, are sampled using the Monte Carlo method [24]. Against the backdrop of time-of-use pricing, the overall load distribution of EVs under both orderly and unregulated charging modes is illustrated in Figure 5.

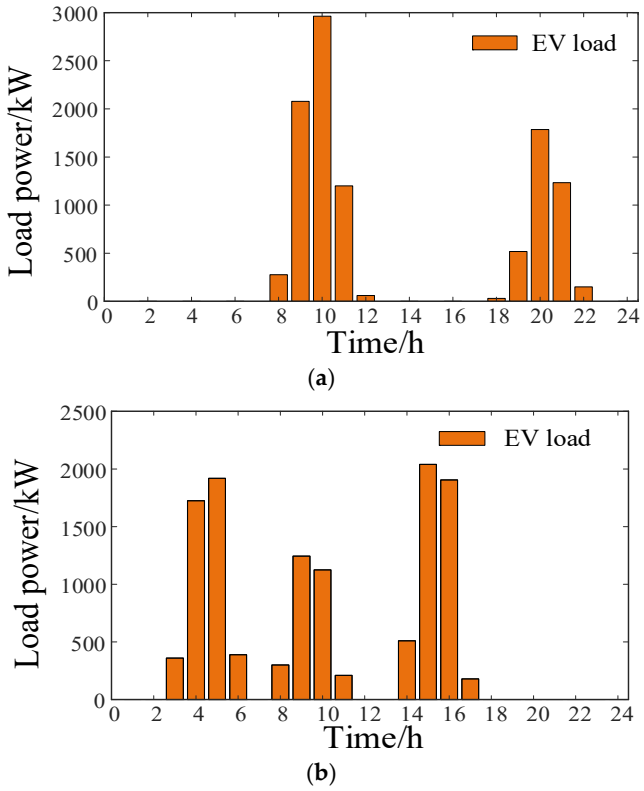

Figure 5. Load Profile of EVs. (**a**) Under unregulated charging mode; (**b**) Under orderly charging mode.

From Figure 5, it is evident that, under the unregulated charging mode, the EV load distribution is relatively random, with a peak load occurring at 10:00 reaching 2962.5 kW. In contrast, under the orderly charging mode, the charging load distribution is more uniform. Influenced primarily by time-of-use pricing, peaks occur mainly during the periods of 3:00–6:00 and 14:00–17:00, with a peak load reaching 2040 kW. This represents a reduction of 922.5 kW compared to the unregulated charging mode, which is approximately 31.34%. This means that the EV load within the microgrid has been effectively managed, reducing the impact of peak loads on the operational safety of the microgrid while also lowering the charging costs for EV users.

5.3. Analysis of P2P Transactions in Microgrids

Comparing microgrid data across cases, Table 2 presents the operational costs of the EV-integrated microgrid, other microgrids, and the multi-microgrid system.

Table 2. Operational costs of the EV-integrated microgrid, other microgrids, and the multi-microgrid system.

Type	Costs of the EV-Integrated Microgrid (USD)	Costs of other Microgrids (USD)	Costs of Multi-Microgrid System (USD)
Case 1	59,252.91	93,638.69	152,891.60
Case 2	37,862.70	68,062.22	105,924.92
Case 3	32,887.35	64,003.50	96,890.85
Case 4	37,570.69	67,789.73	105,360.72
Case 5	32,224.40	63,549.55	95,773.95

In comparison with Cases 1 and 2, the costs in Case 3, as shown in Table 2, are significantly lower across all categories. Specifically, Case 2 reduced the cost of the EV-integrated microgrid by USD 21,390.21 and the multi-microgrid system operating cost

by USD 46,966.68 compared to Case 1. This indicates that DR effectively adjusted the microgrid's load to periods of lower electricity prices, thereby significantly reducing system operating costs. In comparison with Case 2, Case 3 further reduced the operating cost of the EV-integrated microgrid by USD 4975.35 and the multi-microgrid system operating cost by USD 9034.07. This demonstrates that participation in multi-microgrid P2P trading significantly decreases the operating costs of the system.

Case 4 shows a reduction in costs compared to Case 2, indicating that the EV load under the orderly charging mode is more economical than that under the unregulated charging mode. Case 5 presents the lowest cost, demonstrating the advantages of ordered charging, DR, and P2P transactions in enhancing the economic efficiency of the EV-integrated microgrid operation. To investigate the impact of P2P trading on the operation of the EV-integrated microgrid, the operational effects under Case 4 and Case 5 are illustrated in Figures 6–9.

The EV-integrated microgrid described earlier is referred to as Microgrid 1, and the interaction of electricity prices with the other two microgrids is shown in Figure 6. The figure indicates that the interaction of electricity prices between the EV-integrated microgrid and the other two microgrids is relatively low. This is because the core of P2P transactions lies in the collaboration between microgrids. While lower energy interaction costs might reduce the immediate gains of individual microgrids, they allow access to large amounts of inexpensive energy during times of shortage. Therefore, this strategy is quite reasonable for the overall system.

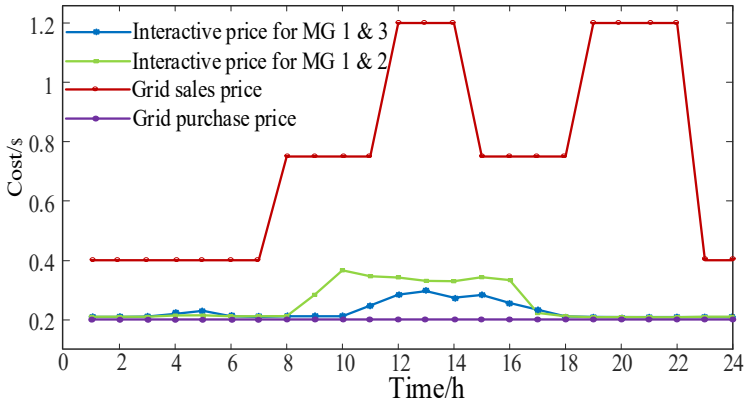

Figure 6. Interaction of electricity prices of Microgrid 1.

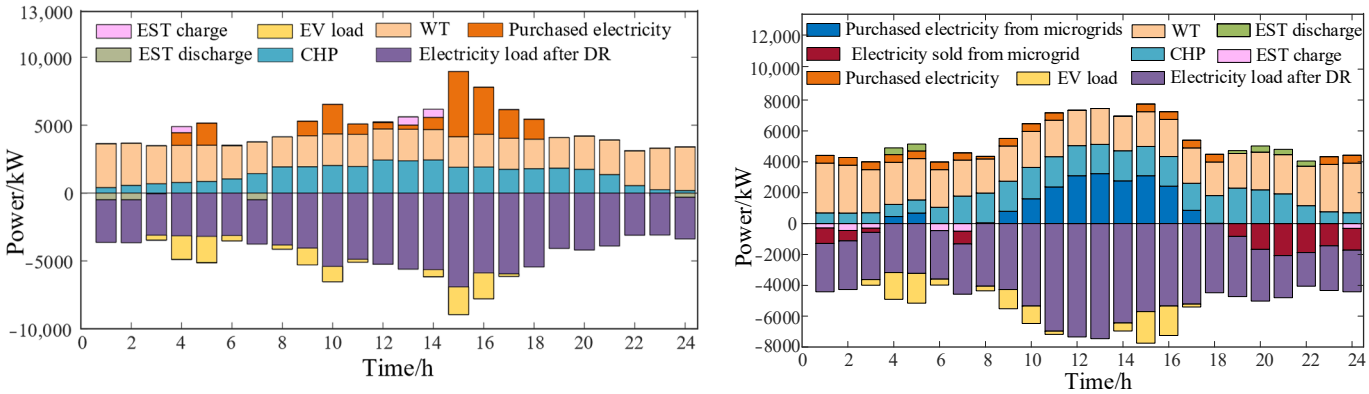

(**a**) (**b**)

Figure 7. Electric equilibrium of the EV-integrated microgrid. (**a**) Without P2P trading conditions; (**b**) Under P2P trading conditions.

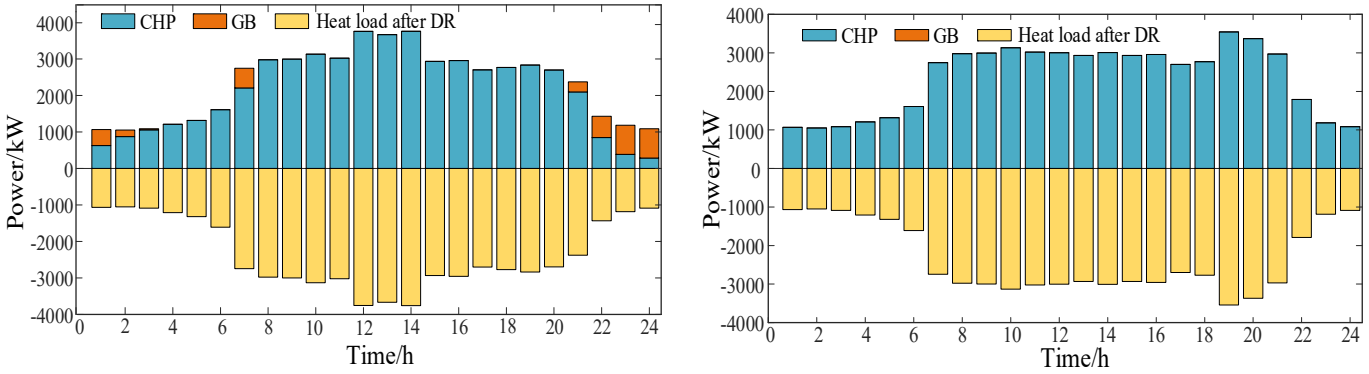

Figure 8. Heat equilibrium of the EV-integrated microgrid. (**a**) Without P2P trading conditions; (**b**) Under P2P trading conditions.

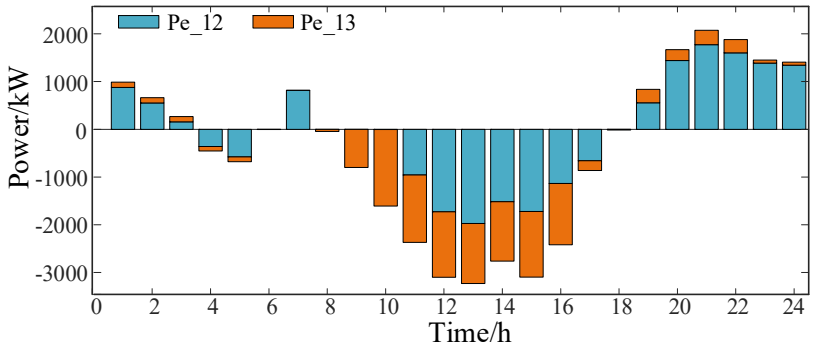

Figure 9. Energy interactions of the EV-integrated microgrid.

Figures 7 and 8 illustrate the electric and heat equilibrium of the EV-integrated microgrid under two scenarios: without the P2P mechanism (Case 4) and with the P2P mechanism (Case 5). Figure 9 specifically addresses the energy interactions of the EV-integrated microgrid.

Comparing Figure 7a,b, it is evident that, during the peak electrical load period from 15:00 to 17:00, the EV-integrated microgrid opts to purchase electricity from other microgrids rather than from the main grid after participating in P2P transactions. This is because, under the P2P trading mechanism, energy exchanges within microgrids are priced lower than the time-of-use electricity rates set by the main grid. Selling excess energy to the grid is less favorable compared to this approach, which better aligns with the overall needs of the multi-microgrid system.

Comparing Figure 8a,b, it can be observed that, after engaging in P2P transactions, the EV-integrated microgrid sells some electricity to the other microgrids to enhance profitability, leading to an increase in the output of the CHP system within the microgrid and a reduction in the need for heating production by the GB.

Figure 9 shows that the core of participating in P2P transactions for the EV-integrated microgrid is to generate additional electricity when its own energy supply is sufficient to meet the needs of the other two microgrids. During periods of insufficient energy supply and high electricity prices, such as from 09:00 to 18:00, it strategically buys a small amount of low-priced electricity from the other two microgrids to reduce the overall operating costs.

To compare and analyze the actual effects of P2P transactions in the multi-microgrid system, Figure 10 illustrates the changes in power load for Microgrid 2 and Microgrid 3 before and after participating in P2P transactions.

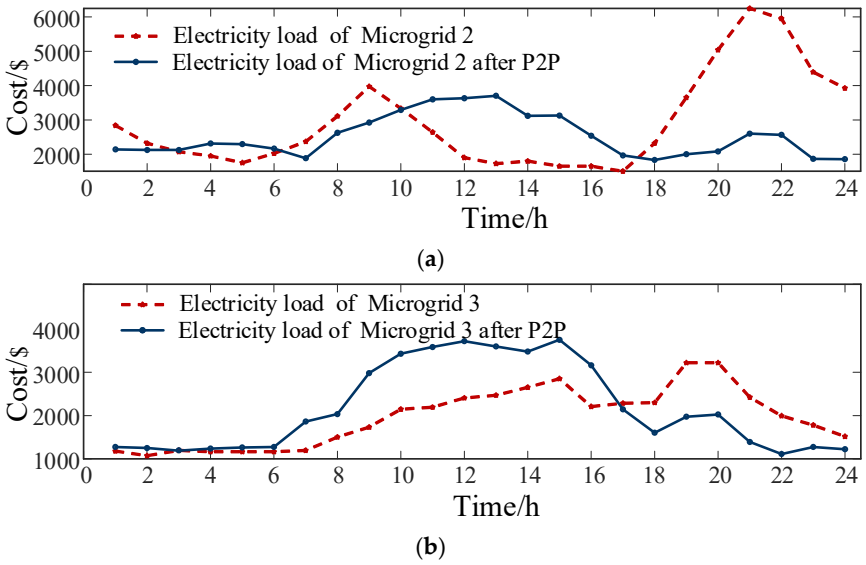

Figure 10. Changes in power load before and after participating in P2P transactions. (**a**) Microgrid 2; (**b**) Microgrid 3.

As shown in Figure 10, the overall load adjustment trends for Microgrid 2 and Microgrid 3 align with the effects presented in Figure 9. From 9:00 to 17:00, the EV-integrated microgrid experiences a peak load that significantly exceeds its own renewable energy output. During this period, Microgrid 2 and Microgrid 3 have some capacity for adjustment, meaning that their internal systems can generate additional electricity to supply the EV-integrated microgrid, thereby reducing the overall operational costs. From 19:00 to 24:00, the power load demand of Microgrid 2 and Microgrid 3 exceeds that of the EV-integrated microgrid. Consequently, to ensure the stable operation of Microgrid 2 and Microgrid 3 while meeting their own load demands, the CHP output of the EV-integrated microgrid continues to increase.

5.4. Convergence of the Strategy

To validate the effectiveness of the proposed strategy, the convergence curves of the cost iterations for the EV-integrated microgrid and the multi-microgrid system are shown in Figures 11 and 12.

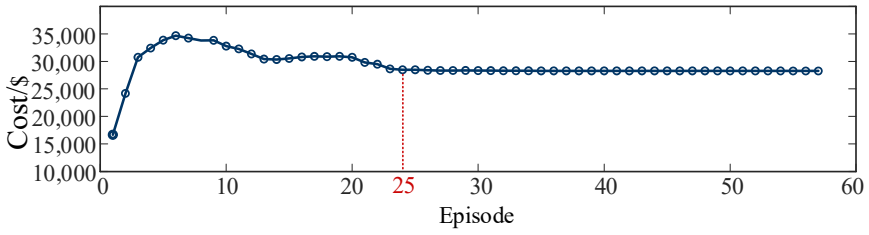

Figure 11. Convergence curves of the cost iterations for the EV-integrated microgrid.

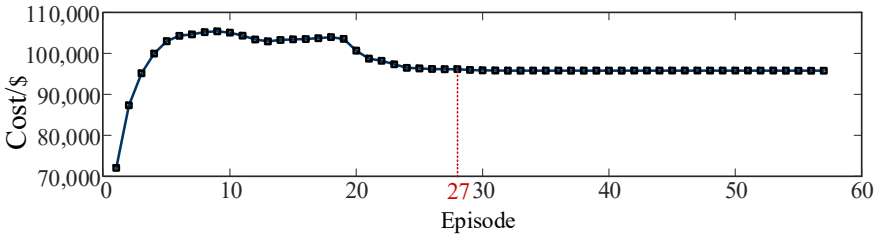

Figure 12. Convergence curves of the cost iterations for the multi-microgrid system.

Figure 11 shows that the cost iteration for the EV-integrated microgrid converges after 25 episodes. Meanwhile, Figure 12 demonstrates that the overall cost iteration for the multi-microgrid system converges after 27 iterations. These results indicate that the strategy proposed in this paper exhibits strong performance.

To verify the applicability of the proposed strategy under different grid conditions, the proportion of renewable energy in the overall load is set at 30%, 60%, and 90%. The convergence curves of the cost iterations for the EV-integrated microgrid and the multi-microgrid system are shown in Figures 13 and 14.

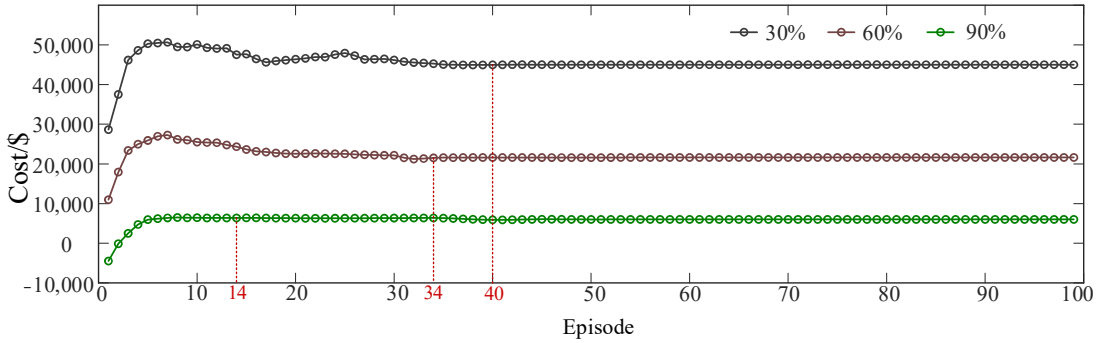

Figure 13. Convergence curves of the cost iterations under varying proportions of renewable energy integration for the EV-integrated microgrid.

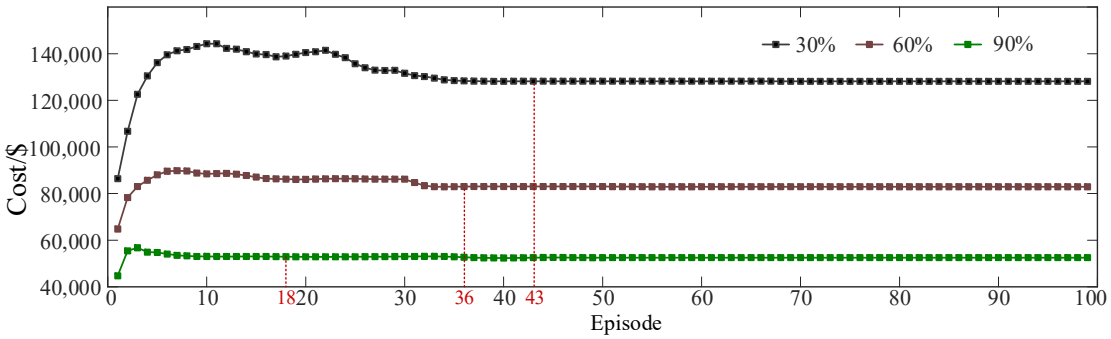

Figure 14. Convergence curves of the cost iterations under varying proportions of renewable energy integration for the multi-microgrid system.

Figure 13 shows that, with renewable energy shares of 30%, 60%, and 90%, the EV integration solutions for the EV-integrated microgrid converge after 40, 34, and 14 iterations, respectively. As the proportion of renewable energy increases, the system's operational costs decrease correspondingly, and the output from equipment is reduced. In certain periods, renewable energy output can fully cover the load, thereby simplifying the solution process and enhancing the convergence speed.

Figure 14 shows that, with renewable energy shares of 30%, 60%, and 90%, the EV integration solutions for multi-microgrid system converge after 43, 36, and 18 iterations, respectively. The overall solution results are consistent with those shown in Figure 13.

6. Conclusions

To explore the dispatch potential of EV load and enhance the economic efficiency of the EV-integrated microgrid, this paper proposes an optimization strategy for EV-integrated microgrids considering P2P transactions. In the context of large-scale EV integration and the incorporation of renewable energy sources, this strategy enhances the economic efficiency and security of microgrid operations, thereby supporting their sustainable development. To validate the effectiveness and superiority of the proposed strategy, simulation verification was conducted, leading to the following conclusions:

(1) Compared to the unregulated charging mode, the proposed framework can reduce EV load peaks by approximately 31.34% and mitigate the impact of EV loads on microgrid operational security.
(2) Compared to running stand-alone strategies, the proposed strategy reduced the operational costs of a single EV-integrated microgrid by approximately 45.61%. For the multi-microgrid system, the operational costs were reduced by 37.36%. This approach not only offers improved economic efficiency, but also ensures the fair distribution of benefits among the microgrids.
(3) Compared to traditional grid-connected modes, the EV-integrated microgrid can generate more profit through energy exchange. The proposed strategy significantly improved the operational conditions within the EV-integrated microgrid. Additionally, the peak load of EV-integrated Microgrid 2 was reduced by approximately 40.75%.

As the capacity of energy storage and demand-side adjustable resources continues to increase, research on the sustainability of microgrid operations will become increasingly significant, our future research will focus on the more detailed operational optimization of multi-microgrid systems.

Author Contributions: Validation, R.T. and J.M.G.; Formal analysis, T.L. and Y.J.; Writing—original draft, S.T.; Writing—review and editing, S.T., T.L. and Q.X.; Supervision, Y.M., H.J. and W.L. All authors have read and agreed to the published version of the manuscript.

Funding: This work was supported by the National Natural Science Foundation of China (No. 52477117, 52107121, 52407135, U2066213, 52222704), State Key Laboratory of Reliability and Intelligence of Electrical Equipment, Hebei University of Technology (No. EERI_KF2021008), Guangdong Basic and Applied Basic Research Foundation (No. 2022A1515240047), China Postdoctoral Science Foundation (No. 2023TQ0242), Youth Talent Program of the China Association for Science and Technology (No. XMSB20240711043), Tianjin Enterprise Science and Technology Commissioner Project (No. 23YDTPJC00090), and Seed Foundation of Tianjin University (No. 2024XHX-0028).

Institutional Review Board Statement: Not applicable.

Informed Consent Statement: Not applicable.

Data Availability Statement: The data presented in this study are available on request from the corresponding author.

Conflicts of Interest: The authors declare no conflicts of interest.

References

1. Cao, J.; Crozier, C.; McCulloch, M.; Fan, Z. Optimal design and operation of a low carbon community based multi-energy systems considering EV integration. *IEEE Trans. Sustain. Energy* **2019**, *10*, 1217–1226. [CrossRef]
2. Cabana-Jiménez, K.; Candelo-Becerra, J.E.; Sousa Santos, V. Comprehensive analysis of microgrids configurations and topologies. *Sustainability* **2022**, *14*, 1056. [CrossRef]
3. Zhao, Y.; Jiang, Z.; Chen, X.; Liu, P.; Peng, T.; Shu, Z. Toward environmental sustainability: Data-driven analysis of energy use patterns and load profiles for urban electric vehicle fleets. *Energy* **2023**, *285*, 129465. [CrossRef]
4. Galvan, E.; Mandal, P.; Chakraborty, S.; Senjyu, T. Efficient energy-management system using a hybrid transactive-model predictive control mechanism for prosumer-centric networked microgrids. *Sustainability* **2019**, *11*, 5436. [CrossRef]
5. Sausen, J.P.; Abaide, A.R.; Vasquez, J.C.; Guerrero, J.M. Battery-conscious, economic, and prioritization-based electric vehicle residential scheduling. *Energies* **2022**, *15*, 3714. [CrossRef]
6. Xiao, Q.; Li, T.; Jia, H.; Mu, Y.; Jin, Y.; Qiao, J.; Pu, T.; Blaabjerg, F.; Guerrero, J.M. Electrical Circuit Analogy-Based Maximum Latency Calculation Method of Internet Data Centers in Power-Communication Network. *IEEE Trans. Smart Grid* 2024, *early access*. [CrossRef]
7. Liu, N.; Chen, Q.; Liu, J.; Lu, X.; Li, P.; Lei, J.; Zhang, J. A heuristic operation strategy for commercial building microgrids containing EVs and PV system. *IEEE Trans. Ind. Electron.* **2015**, *62*, 2560–2570. [CrossRef]
8. Masrur, H.; Shafie-Khah, M.; Hossain, M.J.; Senjyu, T. Multi-energy microgrids incorporating EV Integration: Optimal design and resilient operation. *IEEE Trans. Smart Grid* **2022**, *13*, 3508–3518. [CrossRef]
9. Marcelino, C.G.; Leite, G.M.C.; Jiménez-Fernández, S.; Salcedo-Sanz, S. An improved C-DEEPSO algorithm for optimal active-reactive power dispatch in microgrids with electric vehicles. *IEEE Access* **2022**, *10*, 94298–94311. [CrossRef]

10. Huang, Q.; Jia, Q.; Guan, X. Robust scheduling of EV charging load with uncertain wind power integration. *IEEE Trans. Smart Grid* **2018**, *9*, 1043–1054. [CrossRef]
11. Tan, M.; Ren, Y.; Pan, R.; Wang, L.; Chen, J. Fair and efficient electric vehicle charging scheduling optimization considering the maximum individual waiting time and operating cost. *IEEE Trans. Veh. Technol.* **2023**, *72*, 9808–9820. [CrossRef]
12. Saner, C.B.; Trivedi, A.; Srinivasan, D. A cooperative hierarchical multi-agent system for EV charging scheduling in presence of multiple charging stations. *IEEE Trans. Smart Grid* **2022**, *13*, 2218–2233. [CrossRef]
13. Wu, W.; Lin, Y.; Liu, R.; Li, Y.; Zhang, Y.; Ma, C. Online EV charge scheduling based on time-of-use pricing and peak load minimization: Properties and efficient algorithms. *IEEE Trans. Intell. Transp. Syst.* **2022**, *23*, 572–586. [CrossRef]
14. Aljohani, T.M.; Ebrahim, A.F.; Mohammed, O.A. Dynamic real-time pricing mechanism for electric vehicles charging considering optimal microgrids energy management system. *IEEE Trans. Ind. Appl.* **2021**, *57*, 5372–5381. [CrossRef]
15. Wang, Y.; Qiu, D.; Sun, X.; Bie, Z.; Strbac, G. Coordinating multi-energy microgrids for integrated energy system resilience: A multi-task learning approach. *IEEE Trans. Sustain. Energy* **2024**, *15*, 920–937. [CrossRef]
16. Zhao, Z.; Guo, J.; Luo, X.; Lai, C.; Yang, P.; Lai, L.; Li, P.; Guerrero, J.; Shahidehpour, M. Distributed robust model predictive control-based energy management strategy for islanded multi-microgrids considering uncertainty. *IEEE Trans. Smart Grid* **2022**, *13*, 2107–2120. [CrossRef]
17. Saatloo, A.M.; Mehrabi, A.; Marzband, M.; Mirzaei, M.A.; Aslam, N. Local energy market design for power and hydrogen-based microgrids considering a hybrid uncertainty controlling approach. *IEEE Trans. Sustain. Energy* **2024**, *15*, 398–413. [CrossRef]
18. Liu, Y.; Wang, Y.; Li, Y.; Gooi, H.B.; Xin, H. Multi-agent based optimal scheduling and trading for multi-microgrids integrated with urban transportation networks. *IEEE Trans. Power Syst.* **2021**, *36*, 2197–2210. [CrossRef]
19. Li, Z.; Wu, L.; Xu, Y.; Moazeni, S.; Tang, Z. Multi-stage real-time operation of a multi-energy microgrid with electrical and thermal energy storage assets: A data-driven MPC-ADP approach. *IEEE Trans. Smart Grid* **2022**, *13*, 213–226. [CrossRef]
20. Cao, Y.; Li, D.; Zhang, Y.; Tang, Q.; Khodaei, A.; Zhang, H.; Han, Z. Optimal energy management for multi-microgrid under a transactive energy framework with distributionally robust optimization. *IEEE Trans. Smart Grid* **2022**, *13*, 599–612. [CrossRef]
21. Wang, Y.; Li, Y.; Cao, Y.; Shahidehpour, M.; Jiang, L.; Long, Y.; Deng, Y.; Li, W. Optimal operation strategy for multi-energy microgrid participating in auxiliary service. *IEEE Trans. Smart Grid* **2023**, *14*, 3523–3534. [CrossRef]
22. Yang, Z.; Hu, J.; Ai, X.; Wu, J.; Yang, G. Transactive energy supported economic operation for multi-energy complementary microgrids. *IEEE Trans. Smart Grid* **2021**, *12*, 4–17. [CrossRef]
23. Li, Q.; Liao, Y.; Wu, K.; Zhang, L.; Lin, J.; Chen, M.; Guerrero, J.M.; Abbott, D. Parallel and distributed optimization method with constraint decomposition for energy management of microgrids. *IEEE Trans. Smart Grid* **2021**, *12*, 4627–4640. [CrossRef]
24. Saeed, M.H.; Fang, W.; Kalwar, B.A.; Iqbal, S. A review on microgrids' challenges & perspectives. *IEEE Access* **2021**, *9*, 166502–166517.
25. Li, J.; Khodayar, M.E.; Wang, J.; Zhou, B. Data-driven distributionally robust co-optimization of P2P energy trading and network operation for interconnected microgrids. *IEEE Trans. Smart Grid* **2021**, *12*, 5172–5184. [CrossRef]
26. Qiu, H.; Gu, W.; Xu, Y.; Yu, W.; Pan, G.; Liu, P. Tri-level mixed-integer optimization for two-stage microgrid dispatch with multi-uncertainties. *IEEE Trans. Power Syst.* **2020**, *35*, 3636–3647. [CrossRef]
27. Van, R.J.; Leemput, N.; Geth, F.; Büscher, J.; Salenbien, R.; Driesen, J. Electric vehicle charging in an office building microgrid with distributed energy resources. *IEEE Trans. Sustain. Energy* **2014**, *5*, 1389–1396. [CrossRef]
28. Choobineh, M.; Silva-Ortiz, D.; Mohagheghi, S. An automation scheme for emergency operation of a multi-microgrid industrial park. *IEEE Trans. Ind. Appl.* **2018**, *54*, 6450–6459. [CrossRef]
29. Lu, W.; Xiao, Q.; Jia, H.; Jin, Y.; Mu, Y.; Zhu, J.; Shen, C.; Teodorescu, R.; Guerrero, J.M. A Projected Gradient Descent-Based Distributed Optimal Control Method of Medium-Voltage DC Distribution System Considering Line Loss. *IEEE Trans. Power Syst.* 2024, *early access*. [CrossRef]
30. Zahraoui, Y.; Korõtko, T.; Rosin, A.; Zidane, T.E.K.; Agabus, H.; Mekhilef, S. A competitive framework for the participation of multi-microgrids in the community energy trading market: A case study. *IEEE Access* **2024**, *12*, 68232–68248. [CrossRef]
31. Yuan, Z.P.; Li, P.; Li, Z.L.; Xia, J. Data-driven risk-adjusted robust energy management for microgrids integrating demand response aggregator and renewable energies. *IEEE Trans. Smart Grid* **2023**, *14*, 365–377. [CrossRef]
32. Hannan, M.A.; Lipu, M.S.H.; Hussain, A.; Mohamed, A. A review of lithium-ion battery state of charge estimation and management system in electric vehicle applications: Challenges and recommendations. *Renew. Sustain. Energy Rev.* **2017**, *78*, 834–854. [CrossRef]
33. Xu, J.; Xiao, Q.; Jia, H.; Mu, Y.; Jin, Y.; Lu, W.; Ma, S. A Simplified Control Parameter Optimisation Method of the Hybrid Modular Multilevel Converter in the Medium-Voltage DC Distribution Network for Improved Stability under a Weak AC System. *IET Energy Syst. Integr.* 2024, *to be published*. [CrossRef]
34. Chen, J.; Mao, L.; Liu, Y.; Wang, J.; Sun, X. Multi-objective optimization scheduling of active distribution network considering large-scale electric vehicles based on NSGAII-NDAX algorithm. *IEEE Access* **2023**, *11*, 97259–97273. [CrossRef]
35. Dai, W.; Wang, C.; Goh, H.H.; Zhao, J.; Jian, J. Hosting capacity evaluation method for power distribution networks integrated with electric vehicles. *J. Mod. Power Syst. Clean Energy* **2023**, *11*, 1564–1575. [CrossRef]
36. Xiao, Q.; Yu, H.; Jin, Y.; Jia, H.; Mu, Y.; Liu, H.; Li, W.; Teodorescu, R.; Blaabjerg, F. A novel fault-tolerant operation approach for cascaded H-bridge converter-based battery energy storage systems to avoid overcharge. *IEEE Trans. Ind. Electron.* 2024, *early access*.

37. Wu, Y.; Yu, T.; Pan, Z. A behavior-based and fast convergence energy sharing mechanism for prosumers community. *IEEE Trans. Smart Grid* **2024**, *15*, 4023–4037. [CrossRef]
38. Xiao, Q.; Jin, Y.; Jia, H.; Tang, Y.; Cupertino, A.F.; Mu, Y.; Teodorescu, R.; Blaabjerg, F.; Pou, J. Review of fault diagnosis and fault-tolerant control methods of the modular multilevel converter under submodule failure. *IEEE Trans. Power Electron.* **2023**, *38*, 12059–12077. [CrossRef]
39. Violante, W.; Cañizares, C.A.; Trovato, M.A.; Forte, G. An energy management system for isolated microgrids with thermal energy resources. *IEEE Trans. Smart Grid* **2020**, *11*, 2880–2891. [CrossRef]
40. Liu, J.; Yu, S.S.; Hu, H.; Zhao, J.; Trinh, H.M. Demand-side regulation provision of virtual power plants consisting of interconnected microgrids through double-stage double-layer optimization. *IEEE Trans. Smart Grid* **2023**, *14*, 1946–1957. [CrossRef]
41. Li, J.; Zou, W.; Yang, Q.; Wei, Z.; He, H. A dynamic heat/power decoupling strategy for the fuel cell CHP in the community energy system: A real case study in south of china. *IEEE Trans. Smart Grid* **2023**, *14*, 378–387. [CrossRef]
42. Hou, J.; Zhai, Q.; Zhou, Y.; Guan, X. A fast solution method for large-scale unit commitment based on lagrangian relaxation and dynamic Programming. *IEEE Trans. Power Syst.* **2024**, *39*, 3130–3140. [CrossRef]